Protist, Vol. 172, 125793, February 2021
http://www.elsevier.de/protis
Published online date 29 January 2021

Protist

ORIGINAL PAPER

Erection of a New Genus and Species for the Pathogen of Hard Clams 'Quahog Parasite Unknown' (QPX): *Mucochytrium quahogii* gen. nov., sp. nov.

Sabrina Geraci-Yee[1], Christopher J. Brianik[1], Ewelina Rubin[2], Jackie L. Collier, and Bassem Allam[3]

School of Marine and Atmospheric Sciences, Stony Brook University, Stony Brook, NY 11794-5000, USA

Submitted June 11, 2020; Accepted January 22, 2021
Monitoring Editor: Michael Melkonian

Quahog Parasite Unknown (QPX) is a facultative parasite of the hard clam, *Mercenaria mercenaria*. Although it has been observed in clams since the 1960's and cultivated since the 1990's, conflicting reports on important aspects of its biology have prevented its formal description. 18S rRNA gene sequences identify QPX as a thraustochytrid, but its production of copious mucus is atypical for this group. There are also conflicting reports about whether QPX shares common features of thraustochytrids, such as the production of an ectoplasmic net and biflagellate zoospores. This study reaffirms the previous descriptions of zoospore production by QPX in culture, in multiple strains from several geographic locations, and provides detail on how to maintain QPX cultures under conditions that promote the production of zoospores. Furthermore, we describe new aspects of the life cycle not previously observed. Finally, we erect *Mucochytrium quahogii* gen. nov., sp. nov. to accommodate this unusual thraustochytrid.

Key words: *Mercenaria mercenaria*; stramenopile; Labyrinthulomycetes; thraustochytrid; life cycle; zoospores.

Introduction

Quahog Parasite Unknown (QPX) is a protozoan pathogen of the hard clam, *Mercenaria mercenaria*, that has been credited with causing numerous mass mortality events in hard clams, leading to millions of dollars in losses and even the closure of fisheries (Fig. 1A) (Dove et al. 2004; Drinnan and Henderson 1963; Ragone-Calvo et al. 1998; Smolowitz et al. 1998; Whyte et al. 1994). Although the first appearance of this parasite was reported in 1959 in New Brunswick, Canada, after a mass mortality event (Drinnan and Henderson 1963), it was not until 1989 that it was referred to as QPX and recognized as the causative agent of disease (Kleinschuster et al. 1998; Whyte et al. 1994). Re-infection experiments have been successful in causing disease in naïve clams through injection of

[1]Joint first authors
[2]Present address: Cooperative Institute for Marine and Atmospheric Studies, University of Miami, 4600 Rickenbacker Causeway, Miami, FL, USA 33149
[3]Corresponding author
e-mail bassem.allam@stonybrook.edu (B. Allam).

https://doi.org/10.1016/j.protis.2021.125793

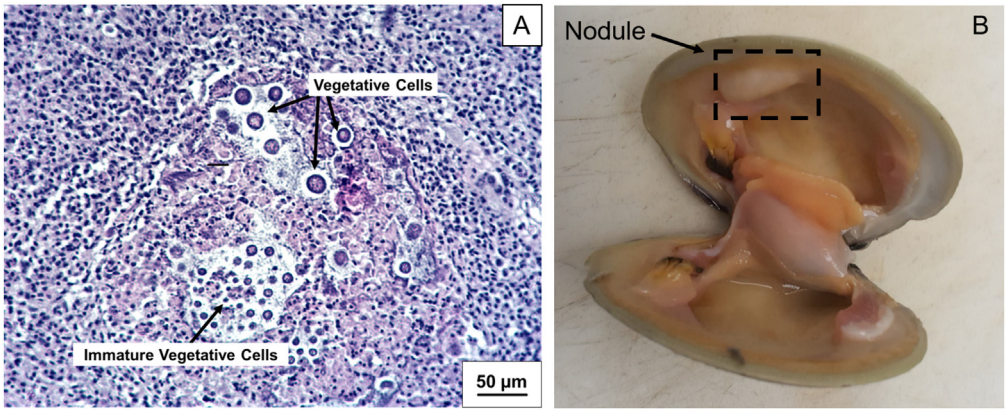

Figure 1. Photomicrograph of a histological cross section with hematoxylin and eosin stain (H&E) of hard clam connective tissue with QPX parasite cells, both immature vegetative and vegetative cells, surrounded by translucent halos of QPX mucus in living animals, which are washed away during histological processing (**A**). Large inflammatory nodule in the mantle tissue of a hard clam from which strain QPX strain LI1 was isolated (**B**).

cultured QPX cells (Dahl and Allam 2007), fulfilling Koch's postulates. Additionally, oligonucleotide probes specific for the 18S rRNA gene of cultured QPX were used to confirm that the DNA sequence corresponds to the pathogen observed in paraffin-embedded hard clam tissues using in situ hybridization (Stokes et al. 2002). The geographic range of QPX disease spans the upper east coast of North America, from Canada to Virginia, where QPX has been detected in both wild and aquacultured hard clam populations (Geraci-Yee et al. submitted; Smolowitz 2018). Even though QPX is responsible for numerous hard clam mass mortality events, it is regarded as a facultative pathogen, commonly found in apparently healthy clams and the marine environment in aggregates, seawater, sediment, and macrophytes (Burge et al. 2013; Ford et al. 2002; Gast et al. 2008; Liu et al. 2009; Lyons et al. 2005). Several recent publications have reviewed QPX disease, such as Smolowitz (2018), Geraci-Yee et al. (submitted), and Collier et al. (2017).

QPX is recognized as a member of the family Thraustochytriaceae (thraustochytrids) in the class Labyrinthulomycetes (= Labyrinthulea) of the division (or phylum) Stramenopiles based on 18S rRNA gene sequencing (Maas et al. 1999; Ragan et al. 2000). Despite being isolated from infected clams in the 1990's (Kleinschuster et al. 1998; Whyte et al. 1994) and determined to be a member of the thraustochytrids by 2000, QPX still lacks a formal description due to conflicting reports of its cell biology and life cycle. A generalized life cycle for the thraustochytrids consists of settlement of a typical stramenopilian biflagellate zoospore to produce a vegetative cell (thallus) that grows and divides to produce new vegetative cells (thalli) or a zoosporangium that releases several to dozens of zoospores (Beakes et al. 2015). The primary purpose of the zoospore is thought to be for dispersal. However, QPX in clam tissue and in culture has been described as having only three stages: a thallus, a sporangium, and a mature sporangium (containing non-motile daughter cells called endospores) (Kleinschuster et al. 1998; Smolowitz et al. 1998). However, Whyte et al. (1994) observed developing flagella in transmission electron microscopy (TEM) in QPX nodules from an infected clam, and Kleinschuster et al. (1998) observed zoospore-like cells via light microscopic examination of QPX cultured in sterile seawater. Attempts to replicate those findings were unsuccessful, leading to the conclusion that previous zoospore observations were possibly the results of contamination by other organisms (Brothers et al. 2000; Smolowitz 2018), suggesting that QPX may only reproduce via non-motile endospores.

As a class, the labyrinthulomycetes are united by the presence of one or more bothrosomes (also referred to as sagenogens or sagenogenetosomes), unique organelles associated with fine, branching extensions of the plasma membrane known as ectoplasmic nets (EN) (Perkins 1972). For thraustochytrids, the EN plays a role in cell anchorage and enzymatic degradation of substrates (Raghukumar 2002), which has led some to hypothesize it plays a role in other opportunistic labyrinthulomycete infections (Burge et al. 2013; Collier et al. 2017; Geraci-Yee et al. submitted). Using TEM, Whyte et al. (1994) observed a

bothrosome-like structure in QPX vegetative cells in an infected clam and Kleinschuster et al. (1998) described the formation of ectoplasmic net-like projections when QPX was cultured in sterile seawater. However, a bothrosome or production of EN have not been observed by others (Geraci-Yee et al. submitted; Maas et al. 1999; Smolowitz 2018). All three stages of the described QPX life cycle produce copious mucus, also referred to as mucofilamentous-nets, which is a unique characteristic of QPX (Kleinschuster et al. 1998; Smolowitz 2018; Smolowitz et al. 1998); however, its relationship to typical labyrinthulomycete EN is unknown.

This study builds upon the previous descriptions of QPX in culture, as well as provides ample evidence for the existence of zoospores, observed in multiple strains from several geographic locations, confirming that production of zoospores is a conserved feature of QPX, although it is only detectable under specific conditions. Furthermore, we describe new cell types not previously reported, and present a new perspective on the QPX life cycle along with its formal taxonomic description using the International Code of Nomenclature for algae, fungi, and plants (ICN).

Results

Taxonomy (ICN)

Stramenopiles (division); Labyrinthulomycetes (class); Thraustochytriales (order); Thraustochytriaceae (family); *Mucochytrium quahogii* S. Geraci-Yee & B. Allam gen. nov., sp. nov.

Mucochytrium S. Geraci-Yee & B. Allam gen. nov

Genus name registrations: 102595 (PhycoBank) and IF557960 (Index Fungorum).

Diagnosis: Vegetative cells are globose and produce muco-polysaccharide secretion (mucus) that lack ectoplasmic nets. Sporangium can produce non-motile (endospores) and/or motile spores (biflagellate zoospores) depending on culturing conditions with two sporulation pathways. Cyst and protoplast stages are present. An amoeboid (motile) stage or production of a proliferous body were not observed. Distinguished from other genera based on molecular inference, production of mucus, and parasitism of hard clams.

Type species: *Mucochytrium quahogii* S. Geraci-Yee & B. Allam sp. nov.

Species assignable: To our knowledge, there are no other species that match the diagnosis.

Etymology: *Muco* = mucus, in recognition of the type species' unique mucus production; *chytrium* = pot, in recognition of the type nomenclature used for naming genera of thraustochytrids.

Mucochytrium quahogii S. Geraci-Yee & B. Allam sp. nov

Species name registrations: 102596 (PhycoBank) and IF557969 (Index Fungorum).

Diagnosis: Vegetative cells (thalli) 2-10 μm, and sporangia (sori) 10-120 μm, are globose and suspended in muco-polysaccharide secretion. Thalli do not attach to pollen grains and lack a rhizoidal ectoplasmic net. Two sporulation pathways exist, both of which produce non-motile spores (immature vegetative cells) and motile zoospores. In the first pathway daughter cells (endospores and zoospores) are produced internally, then released via fragmentation of the sporangial wall (sporangium type 1). In the second pathway, dissolution of the cell wall is followed by rapid budding of the mature sporangium, resulting in successive equal or unequal division of the multinucleate protoplasm, releasing both zoospores and non-motile spores concurrently (sporangium type 2). Daughter cells of this pathway often remain connected by cytoplasmic strands. Zoospores and type 2 sporangia are only observed in cultures washed free of mucus. Biflagellate zoospores are ovoid, 1-2 × 2-3 μm (width × length) with flagella of unequal length, typical of thraustochytrids. Cyst stages are present, characterized by a thickened cell wall that may be either stratified or unstratified, and ranging in size from 30 to 70 μm. Short lived protoplast stages are observed and only present when leaving the thickened cell wall of the cyst stage. Motility of protoplasts or an amoeboid stage were not observed. The species is cryopreserved in a metabolically inactive state by deep-freezing (reference provided below). The species' 18S rRNA gene sequence is deposited in GenBank Accession number MT484273.

In the hard clam host, only the sporangium type 1 pathway, or endosporulation, is observed. Disease is marked by a massive inflammatory response often associated with the necrosis of infected tissues, resulting in poor clam condition and subsequent mortality. Gross signs of disease include swollen, retracted, yellow/tan mantle edges, and yellow/tan inflammatory nodules (blisters or pustules 0.25 to 5 mm in diameter) along the mantle, accompanied with increased amounts of mucus. Primary areas of QPX infection are the mantle, gill, and siphon, with the visceral mass (including

gonads and kidneys), muscle (foot and adductor), and connective tissues involved in advanced cases. Histological examination of infected clams shows vegetative cells often surrounded by translucent halos, which are filled with parasite mucus in living clams that is washed away during the staining process. These halos are free of host cells, and likely formed as QPX digests clam tissue extracellularly or as host cells are physically displaced by QPX mucus production.

Etymology: *quahogii* = Latinized version of the Native American name for hard clams (quahog)

Type host: Hard clam (*Mercenaria mercenaria*)

Holotype: Ex-type strain NY0313808BC7 (abbreviated 8BC7) has been cryogenically preserved and deposited in the American Type Culture Collection (ATCC) as deposit number TSD-50 and is available for purchase.

Holotype locality: Raritan Bay, Staten Island, New York, USA (40.501867, -74.1869)

Paratypes: Strains LI1, MA17, 20AC1, MA (ATCC 50749), VA

Molecular Analyses

All strains used in this study were confirmed to be *M. quahogii* using the QPX-specific PCR assay, which produced the expected 190 bp amplicon. All 18S sequence chromatograms produced from PCR products amplified with universal 18S primers were visually inspected and confirmed the presence of single peaks (no secondary peaks), suggesting there was no contamination from other eukaryotes. Additionally, PCR reactions with universal 16S primers produced two amplification products which were sequenced separately and both of which arose from QPX: an ~ 550 bp PCR product corresponding to the mitochondrial 16S rRNA gene, confirmed by comparison to the newly completed *M. quahogii* genome (Farhat and Allam, unpublished work), and an ~ 700 bp PCR product corresponding to the nuclear 18S rRNA gene, with all sequencing chromatograms containing single peaks. In addition, there was no growth of bacteria observed on marine agar plates, suggesting that the cultures used in our experiments were axenic.

The partial 18S sequences obtained for strains LI1, MA17, and 20AC1 were deposited into GenBank (Table 1) and had 100% sequence identity to the holotype strain 8BC7 (GenBank MT484273). Sequences newly obtained for MA and VA also had 100% sequence identity to their reference sequences in GenBank. In addition to the 18S sequence comparisons in Table 1, the 18S sequence of 8BC7 was identical to 4 *M. quahogii* sequences of other strains in GenBank (%ID = 100% for KX965678, KX965677, DQ641204, AF261664) and differed by one indel from one sequence (%ID = 99.94% for KX965676), while one sequence (%ID = 99.83% for KX965675) differed from all the others at three positions. 18S rRNA gene phylogenetic analyses confirm previous reports on the placement of *M. quahogii* within the thraustochytrids (Fig. 2). Furthermore, the topology and phylogenetic position of *M. quahogii* and its relatives were conserved in all trees using various algorithms (NJ, ME, MP, and ML) with strong bootstrap support (Supplementary Material Fig. S2).

Growth and Staining

M. quahogii strain 8BC7 grew in MEM medium, with or without FBS (see Methods for description of culture medium) following the life cycle previously reported by Kleinschuster et al. (1998), in which a single thallus grows until it becomes a sporangium and endosporulates (Fig. 3, Supplementary Material Video S1), producing large quantities of mucus (Supplementary Material Fig. S1). Growing cells were observed by Nile red staining to accumulate lipids, which were normally concentrated to one side of the cell and proportional with cell size (Supplementary Material Fig. S3A-D). Acriflavine and propidium iodide did not stain *M. quahogii* as expected in comparison to two other thraustochytrids (*Schizochytrium aggregatum* ATCC 28209 and *Aurantiochytrium limacinum* ATCC MYA-1381) used as control organisms. With acriflavine, the entire cell stained green with no red-orange fluorescence of the cell wall (Supplementary Material Fig. S3E, F), regardless of method, fixation, or strain; in addition, we noticed that many cells were not stained. For PI, the entire cell fluoresced red-orange with what appeared to be nuclei concentrating the stain and fluorescing brighter (Supplementary Material Fig. S3G). This was seen for all cells examined for both strains, which was unusual compared to other thraustochytrids that had clearly defined red-orange nuclei (Supplementary Material Fig. S3H). Some large vegetative cells were observed to have large vacuole-like structures with unknown function (Fig. 3A, B). While *M. quahogii* conformed to previous reports when maintained in routine MEM medium, culture manipulation and close observation by time-lapse video microscopy revealed a more complex life cycle than previously recognized and insight into conditions under which different life stages are produced.

Table 1. Details on QPX strains used in this study.

QPX Strain	Isolated from		Isolated on	18S rRNA Gene Sequence			Reference
	Location	Lat, Long		GenBank Accession No.	Length (bp)	%ID to MT484273	
NY0313808BC7 (8BC7)* ATCC TSD-50	Raritan Bay, NY	40.501867, -74.1869	10/31/2003	MT484273	1746	–	This study
LI1	Long Island, NY	Undisclosed	4/23/2019	MT906444	964	100%	This study
MA17	Barnstable, MA	41.709798, -70.320348	10/25/2019	MT906447	975	100%	This study
20AC1	Raritan Bay, NY	40.50625, -74.1526	10/31/2003	MT906446	967	100%	This study
MA ATCC 50749	Cape Cod Bay, MA	Not reported	1997	AF155209	1744	99.94%	Maas et al. 1999
				AY052644	1745	99.94%	Stokes et al. 2002
VA	Old Plantation Creek, VA	37.231442, -75.996817	2009	KX965679 KX965680 KX965681	1750	100%	Rubin et al. 2017
					1750	100%	
					1751	99.94%	

*Holotype.
ATCC = American Type Collection.

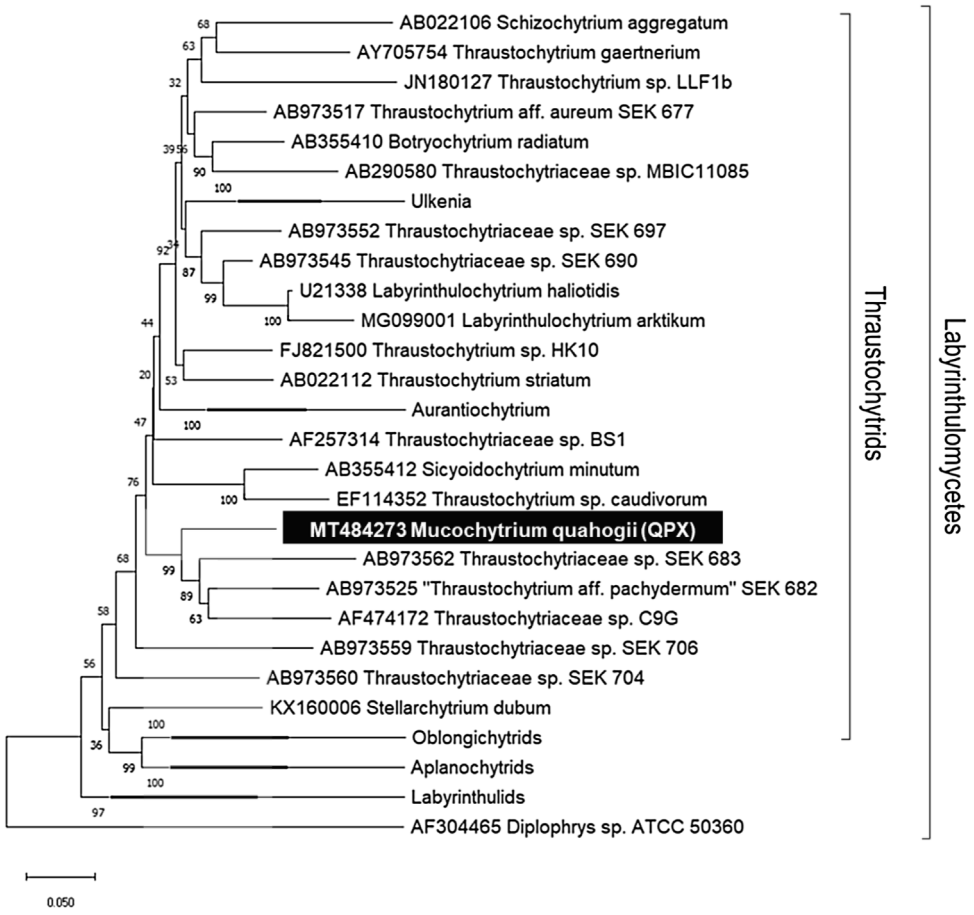

Figure 2. 18S rRNA gene phylogenetic tree showing the position of the *Mucochytrium quahogii* (QPX) strain NY0313808BC7 (8BC7, GenBank sequence MT484273 highlighted) among the labyrinthulomycetes. The tree was constructed in MEGA X using the SILVA r132 alignment (44 sequences) by Neighbor-Joining method with 500 bootstrap replications and 2,247 positions. The number at each node indicates the percent of bootstrap replications in which that node appeared.

Sporangium Type 1

We refer to the life cycle just described, which has been consistently observed in MEM culture with and without FBS (Geraci-Yee et al. submitted; Kleinschuster et al. 1998; Whyte et al. 1994), as the sporangium type 1 pathway (bursting). In short, thalli reaching approximately 3 μm in diameter become multinucleated, continuing to grow until reaching approximately 18 μm in diameter when they undergo cytokinesis, producing distinct endospores in mature sporangia (Fig. 3, Supplementary Material Video S1). There was a direct relationship between cell diameter and number of DAPI-stained nuclei (Cell diameter μm = 0.991 * (# Nuclei) + 4.457, $R^2 = 0.753$) with an average cell diameter of 6.5 μm and an average of 3.65 nuclei per cell (Fig. 5 and Supplementary Material Fig. S4) of the mixed culture harvested during active growth phase (5 to 7 days). It was difficult to count nuclei in cells greater than 20 μm (in diameter) and cells greater than 10 μm (in diameter) did not always have defined nuclei, suggesting nuclear replication. Excluding size, there were no obvious morphological differences between thalli and sporangia until the sporangia began to develop endospores. Mature sporangia in culture released up to 100's of endospores when they burst, depending on the size of the sporangium (Fig. 3). In addition to producing endospores, when washed free of culture mucus and incubated in sterile artificial seawater (SASW), these sporangia were observed to produce both zoospores and endospores from the same mother sporangium (see below). The quantity of zoospores produced varied between sporangia, with some sporangia producing none, while others produced several. The maximum number of zoospores produced by one sporangium was

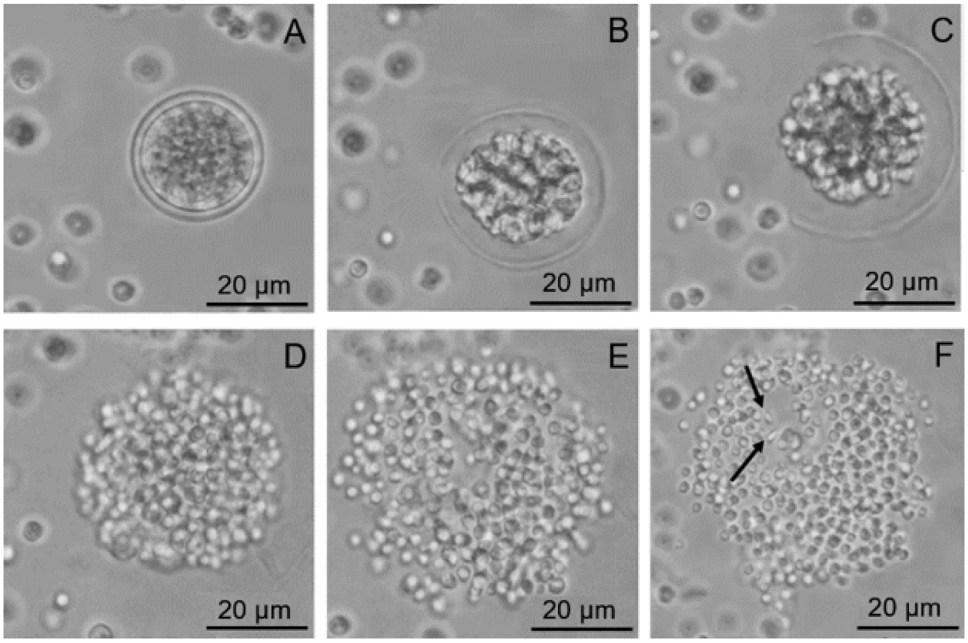

Figure 3. Sporangium type 1 pathway (bursting). This figure depicts the typical endosporulation pathway, although it is from a demucused culture, producing both endospores and zoospores simultaneously. Still microphotographs were taken from the far right of Supplementary Material Video S1, which was recorded at a rate of one image every minute sped up 514 ×. The process pictured above reflects 7.6-hs in real time; corresponding video timestamps, as well as the real time between stages, are provided below. Life stages include mature vegetative cell or thallus developing into a sporangium or sorus (**A**; video timestamp 0:19 s, real time 2 h 49 m), beginning fragmentation of the cell wall (**B**; video timestamp 0:20 s, real time 2 h 51 m), opening of the cell wall (**C**; video timestamp 0:22 s, real time 3 h 8 m), release of endospores (immature vegetative cells produced internally) and zoospores (**D**; video timestamp 0:27 s, real time 3 h 51 m), growth and expansion of endospores and zoospores into surrounding media (**E**; video timestamp 0:46 s, real time 6 h 34 m), two zoospores (pinched cells indicated by arrows) that have opened up space amongst the released endospores (**F**; video timestamp 0:48 s, real time 6 h 51 m).

difficult to estimate due to the limitations of time-lapse photography. Biological variables such as the size of the sporangia, asynchronous timing of the zoosporulation process between sporangia, and the three dimensional environment of the culture further hampered attempts to quantify the maximum amount or proportion of zoospores produced from a single sporangium; regardless, no sporangia were ever observed to produce only zoospores.

Sporangium Type 2

We also observed a previously undescribed pathway that produced zoospores and non-motile spores, which we will refer to as the sporangium type 2 pathway (budding). Both sporangium types (1 and 2) were observed in washed (demucused) cultures, frequently at the same time; however, type 2 sporangia were exclusively observed in washed cultures. Two versions of the type 2 pathway were observed, beginning after dissolution of the cell wall (Supplementary Material Videos S1 and S2). Smaller sporogenous cells (of at least 10 µm in diameter) rapidly underwent multiple, successive (even or uneven) cell divisions (Supplementary Material Fig. S5). In sporogenous cells larger than 10 µm in diameter, the normally smooth, spherical cell became rough and bumpy, leading to multiple cells pinching off simultaneously (Fig. 6). The budding pathway produced a minimum of 16 daughter cells (Supplementary Material Fig. S5F), but much more commonly produced greater than 100 (Fig. 6F), with the number of daughter cells increasing with sporangium size. Successive division was observed in cells that had pinched off from the mother sporangium until all daughter cells were approximately 2-3 µm in diameter (Figs. 4 C-E and 6F). The time required for a type 2 sporangium to completely release daughter cells varied considerably, with some finished in less than an hour (Supplementary Material Video S3) while other

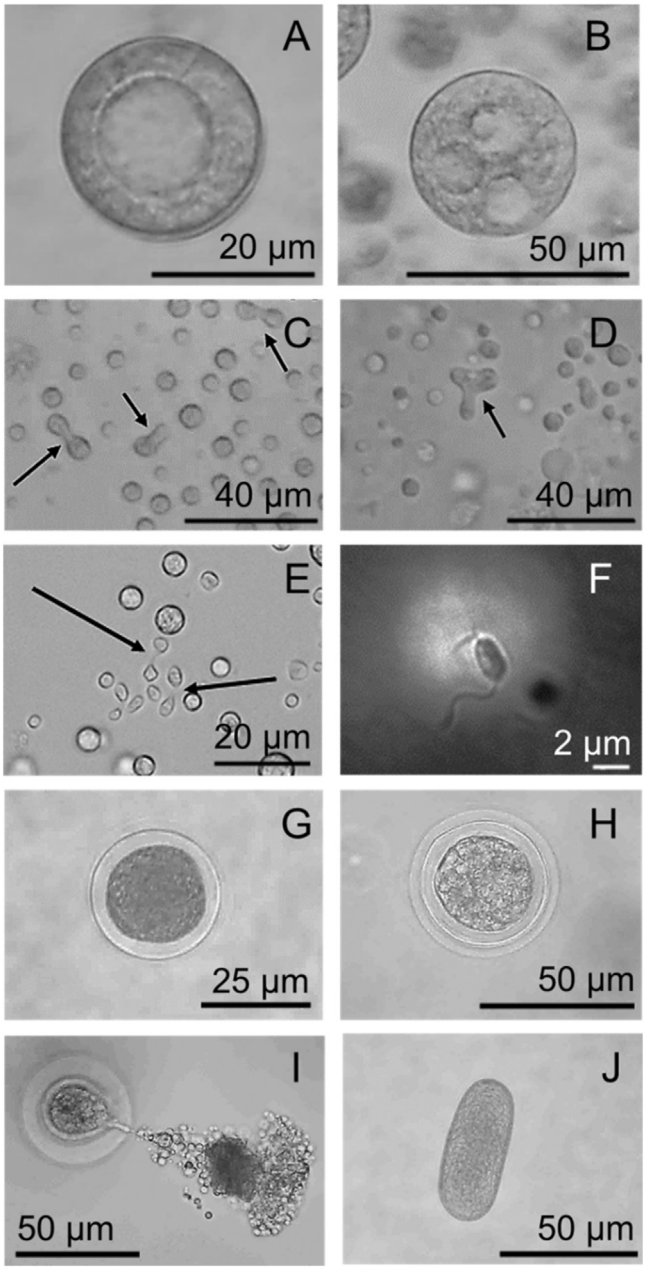

Figure 4. *Mucochytrium quahogii* cells in MEM culture containing vacuole-like structures with unknown function: one vacuole (**A**) and three vacuoles (**B**). Demucused cultured cells in SASW arising from a type 2 sporangium undergoing successive binary (**C**) and ternary division (**D**) indicated by arrows. Still from Supplementary Material Video S3 showing cells remaining connected by a thin cytoplasmic strand after successive budding from a type 2 sporangium indicated by arrows (**E**). Zoospore with two flagella, taken using oil immersion at 1000X (**F**). Cyst stage with thickened, unstratified cell wall of strain 8BC7 (**G**) and stratified cell wall of strain MA17 (**H**), both in MEM media. Variation of the cyst/protoplast immediate division pathway, where division of the protoplasm occurred internally and non-motile spores were formed during release from the cell wall (**I**). Example of a protoplast produced from an encysted cell that rounded out and resumed growth rather than dividing immediately (J). These microphotographs (I, J) are of newly isolated strain MA17 maintained in MEM with 10% FBS.

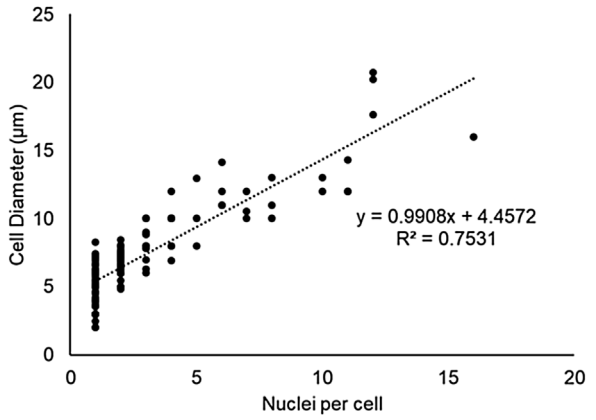

Figure 5. The relationship between cell diameter and number of nuclei per cell, as visualized by DAPI staining (Supplementary Material Fig. S4).

daughter cells were observed to remain connected by cytoplasmic strands for more than 12 hours.

Zoospores

Zoospores were ovoid in shape, between 1-2 μm wide and 2-3 μm long, and had two flagella of unequal length (Fig. 4F, Supplementary Material Video S4). In washed cultures suspended in SASW, the first zoospores appeared after 4 hours of incubation at room temperature, and zoospores remained observable for up to 72 hours, with the most activity usually occurring between 16 and 24 hours after washing. Zoospores were not observed in cultures that were only lightly washed (1 to 3 washes; still contained mucus). Zoospore production was greatest in cells demucused during their active growth phase, typically between 2-5 days after being subcultured and grown on a shaker. Older cultures, between 5 days and 4 weeks, produced fewer zoospores in total and the first zoospores were not detected until 8 to 12 hours after demucusing and incubation in SASW. Zoospores demonstrated no attraction to or preference to settle on pine pollen, clam tissue (adductor muscle and mantle tissue), or sand. The dispersal distances of the zoospores varied considerably, with some zoospores settling adjacent to where they were produced and others settling millimeters away (maximum distance due to the size of the well). During the production of zoospores, other cells in the culture continued to produce mucus, which zoospores would occasionally become stuck in; however, zoospores were still distinguishable from vegetative cells as zoospores could be observed struggling when stuck in mucus. A few zoospores from both type 1 and type 2 sporangia underwent binary division immediately after settling and rounding out (Supplementary Material Video S5). Light did not appear to impact zoospore production. Zoospores were not observed when demucused cells were incubated at low salinity (9 ppt), while cells incubated at moderate and high salinities (17 ppt and 34 ppt, respectively) produced what appeared to be similar amounts of zoospores. Slightly more zoospore production was observed in demucused cells incubated at 13 °C than at colder or warmer temperatures.

Additional Stages

Potential cyst stages, distinguished by thick cell walls that appeared either unstratified (Fig. 4G) or stratified (Fig. 4H), were observed as nutrients became depleted after more than two weeks of growth in culture. Upon the addition of fresh media or suspension in SASW, a small hole appeared in the cell wall. Two possibilities were observed: (1) the cytoplasm of the cell would push out and rapidly start to divide (Fig. 4I, 6, Supplementary Material Video S6), similar to sporangium type 2, producing non-motile spores, or (2) the cytoplasm would flow through, round out and resume typical growth as a thallus (Fig. 4J, Supplementary Material Video S7). The stage responsible for leaving the cyst we will refer to as the protoplast stage due to the changing shape of the cytoplasm observed during this process. There was variation in the two processes just described, and it is likely there are additional excystment processes that were not observed. After the protoplast had escaped, cellular remnants frequently remained in the husk of the old cell wall (Supplementary Material Video S7). Protoplast stages were short lived (a few minutes to 5 hours) and only observed when exiting the thickened cell wall of a cyst. Protoplasts lacked noticeable motility, making it unclear if they represent an amoeboid stage. Production of cysts varied among strains, being observed more frequently in the newly isolated strains (LI1 and MA17) than in the older strain 8BC7, and as a result protoplast stages were more frequently observed in the newly isolated strains.

Life Cycle

The life cycle of *M. quahogii* observed in this study is outlined in Figure 8. A thallus had three possible fates: it could develop into a sporangium type 1, sporangium type 2, or a resting cyst. The most commonly observed pathway was the development of a thallus into a sporangium type 1. In the type 1 pathway a single thallus grows, developing into a mature

sporangium containing endospores, and depending on culture conditions (mucus vs. demucused) released either endospores or both endospores and zoospores. The second pathway, observed only after a culture was demucused, was similar in that a single thallus would grow and develop into a sporangium, however instead of developing internal endospores, a budding-like process released both zoospores and non-motile spores. As cultures aged and nutrients were exhausted (e.g. a two week old culture), some cells would form a cyst stage. After being provided new media, an encysted cell could leave the cell wall through a temporary protoplast stage then resume normal growth into a thallus, or it could leave the cell wall and start dividing rapidly, closely following the second sporangial pathway, but only producing non-motile spores. No evidence of an ectoplasmic net was observed during any stage of the observed life cycle.

Discussion

Our study reveals that the simple life cycle ascribed to *M. quahogii* since it was first cultured (Kleinschuster et al. 1998; Whyte et al. 1994) resulted from limited culturing conditions, and that additional stages are produced under different conditions. In addition to the previously described stages (thallus and sporangium with endospores), we show that *M. quahogii* has a zoospore stage, a cyst stage, a protoplast stage, and a second sporulation pathway (Fig. 8). The sporangium type 1 pathway (Fig. 3) resembles the typical zoosporulation pathway described for most labyrinthulomycetes (Beakes et al. 2015; Yokoyama and Honda 2007; Yokoyama et al. 2007). The sporangium type 2 pathway (Fig. 6 and Supplementary Material Fig. S5) and the cyst/protoplast pathway (Fig. 7) are similar to life stages described for the thraustochytrid genera *Botryochytrium* and *Parietichytrium* (Yokoyama et al. 2007). In these genera, the vegetative cell becomes a protoplast and then an active amoeboid cell, which zoosporulates after "synchronous multipolar budding" characterized by pinching and pulling to produce zoospores (Yokoyama et al. 2007). Daughter cells remaining attached by cytoplasmic strands (Fig. 4E) have also been observed in *Phycophthorum isakeiti* (Hassett 2020) and *Aurantiochytrium acetophilum* (Ganuza et al. 2019), although in the latter case only remaining attached for minutes, whereas in *M. quahogii* the attachment time varied and frequently lasted several hours. Protoplast and amoeboid stages, akin to what we have described, are not unusual for the labyrinthulomycetes, as many species have been reported to produce amoeboid cells and even amoebosporangia from protoplasts (Ganuza et al. 2019; Yokoyama and Honda 2007; Yokoyama et al. 2007). In *M. quahogii*, the emptied cell wall was observed to persist after the release of the protoplast (Fig. 7), similar to the thraustochytrid genera *Ulkenia* and *Parietichytrium* (Yokoyama et al. 2007). In addition, the cysts (Fig. 4G, H) and vacuole-like structures (Fig. 4A, B) observed in this study were similar to those described for *A. acetophilum* (Ganuza et al. 2019).

Life history similarities are also present with the thraustochytrid genus *Monorhizochytrium* (Doi and Honda 2017), in which a general zoosporulation pathway similar to what we describe as the sporangium type 1 pathway of *Mucochytrium quahogii* is also present in all growth conditions examined. Manipulation of culture media also revealed a second pathway in *Monorhizochytrium* similar to the *M. quahogii* sporangium type 2 pathway, consisting of successive binary division prior to zoospore production (Doi and Honda 2017). However, in *Monorhizochytrium*, this second pathway was only observed in organic-enriched liquid media, while in *M. quahogii*, the sporangium type 2 pathway was only observed after demucusing and incubation in nutrient-poor liquid media (i.e. SASW).

Zoospores serve as the primary dispersal mode for most labyrinthulomycetes, including thraustochytrids. The zoospores of *M. quahogii* (Fig. 4F) are of stramenopilian morphology similar to other thraustochytrids (Beakes et al. 2015; Tsu et al. 2012; Yokoyama and Honda 2007; Yokoyama et al. 2007), although *M. quahogii* zoospores were notably smaller than those of *Aurantiochytrium sp.* and *Schizochytrium sp.*, which range between 2.5-7 μm wide and 4-8.5 μm long (Yokoyama and Honda 2007). *M. quahogii* zoospores were similar in size to zoospores of *Althornia crouchii* (2 μm in diameter) (Jones and Alderman 1971), albeit the zoospores of *A. crouchii* were described as spherical in shape rather than ovoid. *M. quahogii* also showed a different response to salinity than *Aurantiochytrium sp.* and *Schizochytrium sp.*, in which zoospore production is typically reduced at salinities above 15 ppt (Tsu et al. 2012). For *M. quahogii*, similar zoospore production and activity were observed at 17 ppt and 34 ppt, while the lower salinity tested (9 ppt) prevented zoosporulation. This is consistent with the general reduction in growth of *M. quahogii* cultures observed at salinities below 15 ppt (Perrigault et al. 2010). *M. quahogii* zoospores were also unusual in showing no attraction to pine

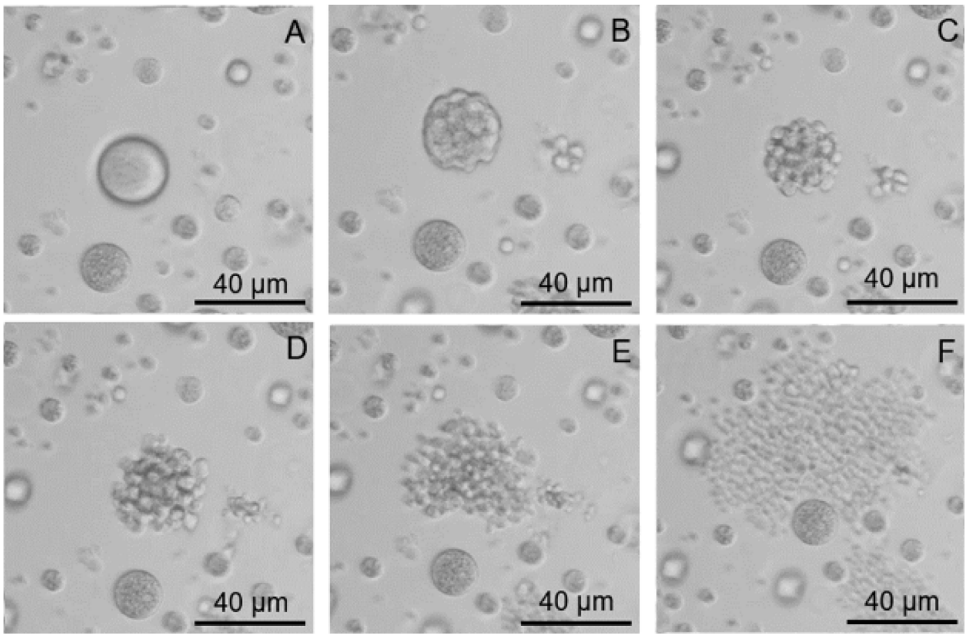

Figure 6. Sporangium type 2 pathway (budding). Still microphotographs were taken from time-lapse video over a 2-h period. A mature sporangium (**A**; 0 m) begins the budding process through dissolution of the cell wall and becomes bumpy (**B**; 15 m). The cell further differentiates (**C**; 20 m) and daughter cells begin to pinch off (**D**; 28 m), eventually settling out while the mother sporangium continues to produce more daughter cells (**E**; 36 m). At the end of the process, all daughter cells are approximately 2 µm (**F**; 94 m).

pollen, which is commonly used to bait, isolate, and enumerate labyrinthulomycetes (Raghukumar 2002). Moreover, *M. quahogii* zoospores showed no attraction to clam tissue, supporting its independence from the hard clam and classification as a facultative pathogen (Burge et al. 2013; Collier et al. 2017; Ford et al. 2002; Gast et al. 2008). The occasional division of *M. quahogii* zoospores immediately after settling is another novel finding (Supplementary Material Video S5). The cell division that occurred after zoospore settlement was similar to the successive division that occurred in the sporangium type 2 pathway (Figs. 4C, D, 6, and Supplementary Material Fig. S5), which resembles the "dumbbell-like" binary cell division described for the thraustochytrid genus *Sicyoidochytrium* (Yokoyama et al. 2007); however, in *Sicyoidochytrium*, this binary division only occurred prior to the production of zoospores. Although we do not know the reason for division after zoospore settlement, we speculate that this phenomenon may facilitate establishment on a substrate or in a host.

M. quahogii is unique amongst the labyrinthulomycetes as it is the only known member of the division to produce vast quantities of mucopolysaccharide secretions and one of two genera - along with *Althornia crouchii* - found to lack an ectoplasmic net (EN) and bothrosome, which is a distinguishing feature of the labyrinthulomycetes (Iwata et al. 2017; Jones and Alderman 1971; Raghukumar 2002; Smolowitz 2018). Additionally, both *A. crouchii* and *M. quahogii* can produce an unusually large number of daughter cells from each sporangium, over 100 (Jones and Alderman 1971) compared to reported highs of 67 for *Oblongichytrium* and 64 for *Schizochytrium* (Yokoyama and Honda 2007). Unfortunately, *A. crouchii* cannot be included in molecular phylogenetic analyses because there are no sequences available for it. Despite its morphological resemblance to *M. quahogii*, we can conclude that *A. crouchii* belongs to a separate genus as it lacks the characteristic mucus of *M. quahogii*, produces round zoospores, does not produce endospores, and was not observed to undergo successive division (Jones and Alderman 1971). Amongst the labyrinthulomycetes represented by 18S rRNA gene sequences (Fig. 2 and Supplementary Material Fig. S2), the closest relatives of *M. quahogii* are three thraustochytrids: "*Thraustochytrium pachydermum*" (GenBank AB973525, 86.78% ID to MT484273), strain C9G (GenBank AF474172, 87.34% ID to MT484273), and the

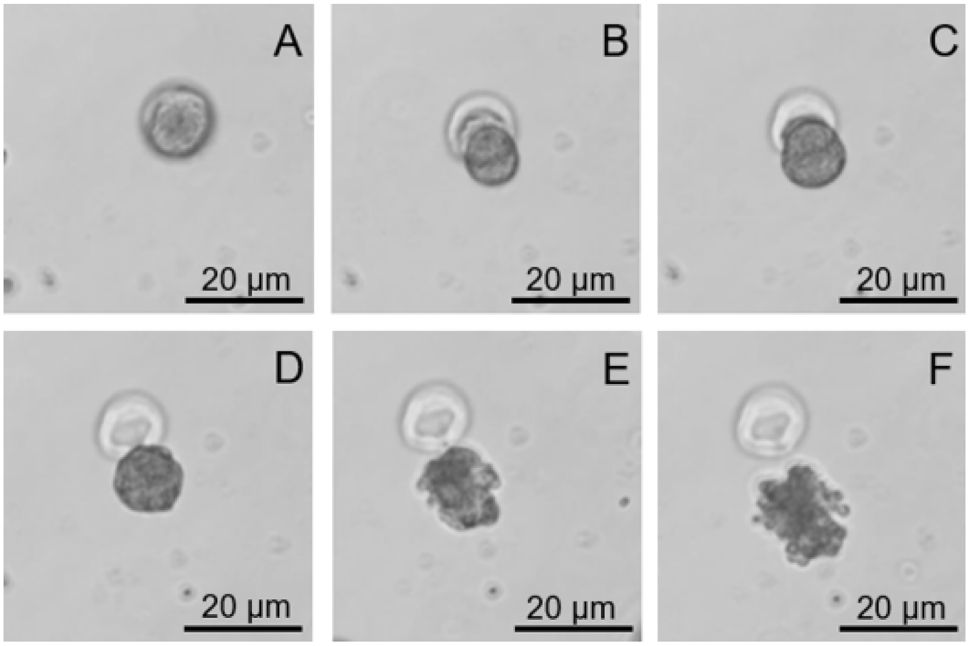

Figure 7. Cyst/Protoplast immediately dividing after leaving the cell wall. Still microphotographs were taken from bottom right quadrant in Supplementary Material Video S6, which reflects 1 hour in real time with one image taken every 40 seconds, sped up 64 × . The protoplast of an encysted cell (**A**; video timestamp 0:07 s, real time 7 m 28 s) begins to flow out of the cell wall (**B**; video timestamp 0:08 s, real time 8 m 32 s). The protoplast continues to exit the cell wall (**C**; video timestamp 0:011 s, real time 11 m 44 s) and becomes bumpy, beginning the budding process (**D**; video timestamp 0:21 s, real time 22 m 24 s). Budding events continue (**E**; video timestamp 0:24 s, real time 25 m 36 s) until daughter cells differentiate and non-motile spores are formed (**F**; video timestamp 0:34 s, real time 36 m 16 s).

strain SEK 683 (GenBank AB973562, 83.9% ID to MT484273). These thraustochytrids have 18S rRNA gene sequences that are less than 90% identical to *M. quahogii* and have not been reported to produce mucus. While *T. pachydermum* shares some similar characteristics with *M. quahogii*, such as general cell morphology with relatively larger sized cells (15-30 µm in diameter), thick cell wall (3-5 µm), and high salinity tolerance (2.5-60 ppt), its zoospores are much larger (3 × 5 µm) and it produces very fine EN (Bowie 1970). The morphology and size of strain C9G, as well as its ability to produce EN and zoospores were not reported, although it is clearly different from *M. quahogii* in sensitivity to clam hemocytes and clam plasma (Anderson et al. 2003). Unfortunately, there are no details on strain SEK 683 (Ueda et al. 2015) other than the 18S rRNA gene sequence.

Further supporting the uniqueness of *M. quahogii* is its unusual staining by common dyes. For the acriflavine stain, *M. quahogii* cell walls did not show the typical red-orange fluorescence seen for other labyrinthulomycetes (Supplementary Material Fig. S3E, F), implying different structure or composition of the cell wall. Whyte et al. (1994) described variation of the cell wall among *M. quahogii* cells; in some it appeared to consist of "fibrous material" more similar to other labyrinthulomycetes, while in others it consisted of a "loose multilaminar structure" considered to be atypical of thraustochytrids but comparable to *Labyrinthulochytrium haliotidis* (Hassett and Gradinger 2018), formerly *Labyrinthuloides haliotidis*, a thraustochytrid pathogen of the juvenile abalone (Bower, 1987a; Whyte et al., 1994). Alternatively, acriflavine may be unable to penetrate the relatively thick cell wall of *M. quahogii*. Regardless of the mechanism, it is clear that the acriflavine direct detection (AfDD) method for enumeration of thraustochytrids (Raghukumar and Schaumann 1993) does not work for *M. quahogii*. Additionally, the PI stain (Supplementary Material Fig. S3G, H) was not effective for the visualization of *M. quahogii* nuclei, but DAPI was used successfully and revealed insights into nuclear replication and sporogenesis (Fig. 5 and Supplementary Material Fig. S4). Nile red revealed that *M. quahogii* possesses lipid droplets that fluoresce yellow-gold (Supplementary Material Fig. S3A-D), consistent

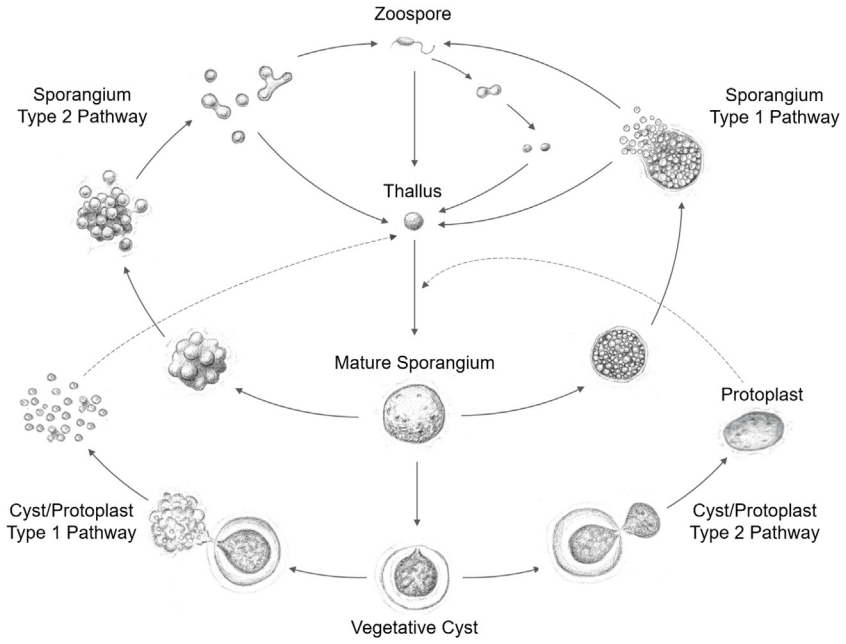

Figure 8. Life cycle of *Mucochytrium quahogii* (not drawn to scale). A thallus (vegetative cell) becomes a mature sporangium, which could follow three pathways, sporangium type 1, sporangium type 2, or become a vegetative cyst. The sporangium type 1 pathway internally produces endospores, which burst free under normal culturing conditions, or produces both endospores and zoospores after demucusing. The sporangium type 2 pathway was only observed after demucusing, resulting in budding of the mature sporangium and production of both non-motile spores and zoospores. Zoospores could settle, round out and resume typical growth or settle and divide before resuming growth into a thallus. Cysts could resume growth by pushing through the cell wall and rapidly start dividing resulting in non-motile spores, or by producing a protoplast that would round out and resume typical growth into a thallus.

with other labyrinthulomycetes (Jeh et al. 2009). The placement of the lipid droplets concentrated to one side of the cell may result from the demucusing and centrifugation procedure; unfortunately, since the demucusing process is needed to stain *M. quahogii* cells, we do not know what the lipid droplets would look like in their natural state. We did notice that larger cells contained proportionally more lipids, which were less concentrated to one side of the cell and expanded toward the center of the cell; perhaps the observed vacuole-like structures contained large lipid droplets.

No other labyrinthulomycete has been described to produce both non-motile endospores and biflagellate zoospores simultaneously from the same sporangium. Some thraustochytrid genera (*Sicyoidochytrium* and *Parietichytriu*m) have been reported to first produce non-motile spores that turn into biflagellate zoospores (Yokoyama et al. 2007) and aplanochytrids (genus *Aplanochytrium*) can produce crawling aplanospores that lack flagella (Leander et al. 2004). We acknowledge that it is possible that zoospores could be consistently produced in culture, but due to their small size, short duration, and interference of their movement by mucus, have gone unnoticed. However, we think this is unlikely as no zoospores were observed in cultures subjected to light washing, implying a complete or near complete removal of mucus is needed to trigger zoosporulation. Furthermore, we have not observed flagella in transmission electron microscopy of cultures grown in MEM with FBS (Allam, unpublished work).

The need for demucusing to trigger the production of zoospores and type 2 sporangia may reflect the habitat *M. quahogii* is adapted to and the role its mucus plays in its ecology. The mucus of *M. quahogii* is thought to contain proteins important in host invasion and disease development, and is considered to be a virulence factor (Garcia-Vedrenne et al. 2013; Rubin et al. 2015, 2016, 2017); however, the mucus may represent a “dual use” virulence factor, promoting survival in the host and environment, as is seen in opportunistic fungal pathogens (Casadevall et al. 2003). When *M. quahogii* is outside of its host in the marine environment, the mucus may play a role in substrate adherence, as the species is commonly found in

the flocculent layer of the sediment-water interface (Geraci-Yee et al., unpublished work) and associated with marine snow and macroalgae (Gast et al. 2008; Lyons et al. 2005). In fact, the mucus of old cultures (>1 month) of *M. quahogii* is usually observed to adhere to the walls of the culturing flask (Supplementary Material Fig. S1C). The mucus of *M. quahogii* may inhibit the production of zoospores, through a mechanism such as a physical trigger or possibly signaling compounds in the mucus, preventing zoospores from being produced as they would be unable to escape from the mucus. Another thraustochytrid pathogen, *L. haliotidis*, also did not zoosporulate in culture unless cells were washed free from the culture medium and incubated in sterile seawater; and in association with the host, zoospores were only observed after vegetative cells were released from degrading host tissue into seawater (Bower 1987b). This may reflect an evolutionary selective pressure on thraustochytrid pathogens, which prevents zoosporulation in nutrient rich habitats (host tissue or culture media) until growth is no longer supported, triggering zoosporulation for dispersal.

The mechanism of *M. quahogii* (QPX) disease transmission in hard clams remains unknown. As a facultative pathogen, it is currently hypothesized that *M. quahogii* pathogenesis occurs only when clams are disadvantaged by "unfavorable gene-environment interactions" (Ford et al. 2002). For example, it is thought that cold temperatures are required for successful infections due to the northern occurrence of the disease, in addition to host immunosuppression at low temperatures, resulting in disease development (Dahl et al. 2011; Perrigault et al. 2011). QPX has been successfully transmitted to naïve seed clams by long-term cohabitation with naturally infected clams from a heavily impacted QPX site, with the highest QPX infection prevalence among naïve clams observed under low temperature (Smolowitz 2018). However, exposing naïve clams to cultivated *M. quahogii* cells via bath exposure has failed to establish disease regardless of temperature (Dahl and Allam 2007; Smolowitz 2018), with only direct injection of cultured *M. quahogii* cells proving successful (Dahl and Allam 2007; Dahl et al. 2008). The necessity of injection for the initiation of disease is unfortunate as physical damage can alter a clam's immune response, and it does not accurately depict how infections are naturally transmitted. However, all previous work on disease transmission has been with *M. quahogii* reared in MEM with FBS, thus only representing typical thalli and sporangium type 1 stages (endospores). Our work raises the possibility that one of the new stages of *M. quahogii* described here may be responsible for infection and pathogenesis, as parasites commonly have specific infective stages (i.e. cercaria of trematodes, sporozoites of *Plasmodium*, promastigotes of *Leishmania*, etc.). Specifically, the motile zoospore stage, as well as type 2 sporangium and cyst/protoplast stages, open up new avenues of research into natural disease transmission and progression.

To summarize, this paper has provided evidence confirming the controversial zoospore stage of *M. quahogii*, as well as describing new aspects of its life cycle in culture. Additionally, we have described the methods required to produce these life stages. Comparisons to other labyrinthulomycetes were drawn elucidating the complex life cycles present in these understudied protists. This study opens the door for future experiments to examine how these new life stages of *M. quahogii* influence its role as a facultative parasite of the hard clam.

Methods

Strains: The strains used for this study are summarized in Table 1. The strain designated as the holotype is NY0313808BC7 (abbreviated 8BC7), which was initially isolated from an infected clam from Raritan Bay, Staten Island, New York (NY), USA on October 31, 2003. Two new strains (LI1 and MA17) obtained from QPX-infected hard clams collected from Long Island, NY and Barnstable, Massachusetts (MA), respectively, were used to validate the observations initially made with 8BC7. Additional strains were used for staining experiments: 20AC1, MA, and Virginia (VA).

QPX isolation: QPX was isolated from inflammatory nodules in the mantle tissue of wild hard clams (Fig. 1B), which are characteristic of QPX disease, using the methods described by Kleinschuster et al. (1998). Briefly, the nodule was aseptically removed from the mantle and surface sterilized with 100% ethanol, after which the nodule tissue was immersed in sterile artificial seawater (SASW, 34 ppt or g/L of Instant Ocean, Spectrum Brands, Blacksburg, VA) to wash away residual ethanol; this washing step was repeated 5 times. The nodule was disrupted with sterile scalpel blades and transferred to 2 ml of culture medium described by Kleinschuster et al. (1998). The culture medium consisted of 5.1 g/L Minimum Essential Medium (MEM) Eagle (α modification, Sigma M0644), 1.82 g/L $CaCl_2$ x 2 H_2O, 0.68 g/L KCl, 4.36 g/L $MgCl_2$ x 6 H_2O, 24.26 g/L NaCl, 3.16 g/L $MgSO_4$ x 7 H_2O, 5 g/L HEPES, 0.5 g/L D + glucose, 100 U/mL penicillin, and 0.1 mg/mL streptomycin supplemented with 10% by volume heat-inactivated fetal bovine serum (FBS; Gibco Performance Plus, ThermoFisher Scientific, Waltham, MA), adjusted to a pH of 7.2 with 1 M NaOH and filter sterilized (0.2 μm). We refer to the QPX culture medium as MEM with FBS, while culture medium MEM contains all the components previously mentioned, not supplemented with FBS. Newly isolated cultures were maintained in MEM with FBS, incubated at 20 °C, and monitored daily for growth.

QPX identification: Successful isolation of QPX was confirmed by microscopy and molecular methods. QPX genomic

DNA (gDNA) was extracted from an aliquot of culture using the NucleoSpin Tissue Genomic DNA extraction kit (Macherey-Nagel, Inc. Bethlehem, PA) following the standard protocol for cultured cells. Extracted gDNA was assessed for quantity and purity by Nanodrop ND-1000 spectrophotometry (Thermo Scientific, Wilmington, Delaware). For QPX confirmation, QPX-specific primers (Liu et al. 2009) were used, as well as universal 18S primers (Collado-Mercado et al. 2010; Medlin et al. 1988), followed by Sanger sequencing of PCR products. Primers were synthesized by Integrated DNA Technologies, Inc. (Coralville, IA). The QPX-specific primers were 5.8S24 For (5'- TTT AGC GAT GGA TGT CT -'3) and QPX-ITS2-R2 (5'- GCC CAC AAA CTG CTC TWT -'3), which targets the ITS region and produces a product of 190 bp (Liu et al. 2009). For the 18S PCR assay, primers 18S Forward (5'- AAC CTG GAT GAT CCT GCC AGT -3') and 18S Reverse (5'- TGA TCC TTC TGC AGG TTC ACC TAC -3'), originally designed by Medlin et al. (1988) and modified by Collado-Mercado et al. (2010) were used. Each 20 μl PCR reaction contained 6.5 μl of nuclease-free water, 2 μl of 25 mM $MgCl_2$, 2 μl of 2 mM dNTPs, 2 μl of 2 μM forward and reverse primers (final concentration 200 nM), 4 μl of 5X GoTaq Flexi buffer (colorless), 0.5 μl GoTaq G2 Flexi DNA Polymerase (Promega, Madison, WI), and 1 μl of template DNA. The PCR program was 40 cycles of 95 °C for 30 seconds, 55 °C for 1 minute, 72 °C for 1 minute and 30 seconds with a final extension at 72 °C for 10 minutes, performed on a Mastercycler gradient thermocycler (Eppendorf, Hamburg, Germany). PCR products were visualized by agarose gel electrophoresis to confirm the expected amplicon size. The 18S PCR products were purified using the NucleoSpin Gel and PCR clean up kit (Macherey-Nagel, Inc. Bethlehem, PA) and Sanger sequenced to obtain a partial 18S sequence (~1000 bp). Cloning and sequencing was used to obtain a nearly full-length 18S rRNA gene sequence for the holotype strain 8BC7, following the methods of Rubin et al. (2017). Additionally, cultures were screened for the presence of contaminants by both universal 16S PCR assays (Teske et al. 1998) and plating culture material on marine agar.

Phylogenetic analyses: The QPX holotype strain 8BC7 18S rRNA gene sequence was aligned with representative labyrinthulomycete sequences obtained from the SILVA database (r132) using ClustalW (Thompson et al. 1994). Phylogenetic analyses were performed on the alignment consisting of 44 nucleotide sequences using MEGA X (Kumar et al. 2018), and phylogenetic trees were generated using Neighbor-Joining (NJ), Minimum Evolution (ME), Maximum Parsimony (MP), and Maximum Likelihood (ML) methods. The NJ tree was constructed using the Maximum Composite Likelihood model with gamma distribution (shape parameter = 1), uniform rates among sites, and pairwise deletion for ambiguous positions with 500 bootstrap replications. The ME tree was constructed using the Maximum Composite Likelihood model with gamma distribution (shape parameter = 1), uniform rates among sites, pairwise deletion for ambiguous positions, and close-neighbor-interchange with 500 bootstrap replications. The MP tree was constructed with complete deletion of gaps or missing data (treatment option) and Subtree-Pruning-Regrafting algorithm using search level 1 with initial trees obtained by the random addition of sequences (10 replicates) with 500 bootstrap replications. The ML tree was constructed using the General Time Reversible model, gamma distributed with invariant sites (5 categories) and nearest-neighbor-interchange. There were 2,247 positions in the final dataset for the NJ, ME and ML analyses and 1,233 positions for the MP analysis.

Culture maintenance: QPX was maintained in MEM (with and without FBS) in vented or unvented culture flasks at 20 °C and 23 °C (Supplementary Material Fig. S1A). Subcultures were performed weekly to bimonthly using 10% inoculum (v/v, 1 ml) into fresh media (10 ml). For experiments, cultures of QPX strain 8BC7 were agitated (orbital shaker at 45 rpm) and grown in vented culture flasks at room temperature (~ 23 °C) in MEM without FBS. QPX grew more rapidly with gentle agitation compared to static cultures and produced less mucus, making it easier to manipulate.

Zoospore production: In order to promote zoosporulation, the abundant mucus produced by the culture must be washed away from the vegetative cells. Maximal zoospore production was observed when a 15% inoculum of QPX stock culture (grown with FBS) was added to fresh MEM without FBS, and then grown on a shaker at 45 rpm for 2-3 days at room temperature. After the incubation period, while the cells were still in active growth phase, the culture was demucused (washed free of mucus) by adding 4 times the culture volume of SASW then passage through a 20-gauge x 1 ½" needle (Supplementary Material Fig. S1B, D). The culture-seawater mixture was then centrifuged at 1,400 x g for 20 minutes. The upper 50% of the supernatant was poured off, as pouring more than 50% would normally result in disturbing the QPX pellet due to the remaining mucus. New SASW was added to replace what had been poured off, and passage through a 20-gauge needle was repeated to resuspend the QPX cells. Washing and centrifugation was repeated 4-5 times until all mucus was removed and cells could be easily pipetted. Subsequent to the last centrifugation, all the remaining supernatant was poured off and the mucus-free QPX cells were resuspended in 10 ml of SASW. For observations, the mucus-free QPX cells were further diluted 4-fold with SASW in 12- or 24-well culture plates, and time-lapse video microscopy performed using a Nikon Eclipse TE 2000-S microscope equipped with NIS-Elements D imaging software.

Following the subculturing and demucusing methods described above, the impacts of culture age, growth media (MEM with or without FBS), light intensity, incubation temperature after washing, and culture salinity on zoospore production were tested. Culture age and growth media were tested concurrently by allowing a culture to grow with shaking either with or without FBS at room temperature (23 °C) for 1, 2, 3, 4, 5, 6, 7, 10, and 14 days before demucusing. The impact of temperature on zoosporulation was tested by incubating demucused cultures at 10, 13, 16, 20, 23, and 25 °C for ~ 20 hours before the culture was observed. In addition, the impact of light on zoosporulation was also examined at these 6 temperatures, with "dark" cultures wrapped in tinfoil. The effect of salinity on zoosporulation was examined using SASW at salinities of 9, 17, and 34 ppt (or g/L of Instant Ocean). Lastly, demucused cultures were tested for attraction to substrates: sterile pine pollen, clam tissue, and sterile sand. After washing, the demucused cells were left to incubate at room temperature for ~ 4 hours and then a small amount (< 1 g) of substrate was added to the culture wells. Cultures were microscopically observed for any immediate chemotactic response, then left to incubate overnight (~ 12 hours) under time-lapse photography to observe any propensity for zoospore attraction and settlement.

Staining QPX: To investigate QPX cell biology, we stained cultured QPX cells with a variety of dyes, including acriflavine, DAPI (4′,6-diamidino-2-phenylindole), propidium iodide (PI), and Nile red. All cultures were grown in MEM with FBS and agitation at room temperature. We also stained other common thraustochytrids (*Schizochytrium aggregatum* ATCC 28209 and *Aurantiochytrium limacinum* ATCC MYA-1381) for comparison. All epifluorescence microscopy was performed using a Leitz Laborlux S microscope with ISCapture software for image acquisition.

Acriflavine. Cultured QPX cells of three strains (8BC7, 20AC1, and MA) were demucused as described above and stained with acriflavine (Raghukumar and Schaumann 1993). The cell wall and nucleus of thraustochytrids are expected to fluorescence differently (orange-red and blue-green, respectively) under blue-light excitation due to the presence of sulfated polysaccharides in the cell wall, distinguishing labyrinthulomycetes from other protists. A modified version of the protocol using centrifugation with and without destaining with 75% isopropanol was also tested. For the centrifugation protocol, a 100 μl aliquot of washed live or formaldehyde-fixed (0.8%) cells in SASW was spun down for 5 minutes at 5,000 x g and the supernatant was removed. Cells were resuspended in 100 μl of 0.05% acriflavine solution (in 0.1 M citrate buffer, pH 3) for 3 minutes. Stained cells were spun for 2 minutes at 5,000 x g and either resuspended in 30 μl of SASW and immediately visualized by epifluorescence microscopy or in 100 μl of 75% isopropanol for the destaining step. To remove isopropanol, cells were spun for 2 minutes at 5,000 x g and resuspended in 30 μl of SASW for visualization by epifluorescence microscopy with a Leitz I3 filter block (excitation BP 450-490 nm; dichroic 510 nm; emission LP 515 nm).

DAPI. Cultured, demucused QPX cells of four strains (8BC7, 20AC1, MA, and VA) were combined and fixed with 0.8% formaldehyde for at least 30 minutes. A 20 μl aliquot of fixed cells was mixed with 10 μl of DAPI (1 μg/mL in 1X phosphate buffered saline) by pipetting and incubated in the dark at room temperature for at least 10 minutes. Stained cells were mounted on a slide and cell diameter and number of nuclei per cell were determined for 146 cells in two independent trials by epifluorescence microscopy with a Leitz A filter block (excitation BP 340-380 nm; dichroic 510 nm; emission LP 425 nm).

Propidium Iodide. Cultured, demucused QPX cells were fixed (70% ethanol) and stained with propidium iodide (PI, 10 μg/mL final concentration), which is a red fluorescent nuclear stain under blue excitation (Pozarowski and Darzynkiewicz 2004). PI staining was performed on QPX strains 20AC1 and MA. A small aliquot was mounted on a slide and visualized using epifluorescence microscopy with a Leitz I3 filter block.

Nile Red. To examine whether QPX accumulates lipid droplets in culture like most thraustochytrids, QPX was stained with Nile red following a modified protocol (Pandey and Bhathena 2014). Live or formaldehyde-fixed (0.8%) demucused QPX cells were spun down and resuspended in SASW. Nile red was added to the cell suspension at 10 μg/mL in 10% DMSO (final concentration). The cell suspension was shielded from light and gently vortexed for 1 minute, then incubated in the dark for 5 minutes. Nile red staining was performed on QPX strains 20AC1 and MA. Cells were mounted on a slide and visualized under epifluorescence microscopy with a Leitz I3 filter block.

Authors Statement

Bassem Allam conceived the study and secured the funding. Jackie Collier contributed to study design and analyzed molecular data. Sabrina Geraci-Yee, Christopher Brianik and Ewelina Rubin collected experimental data. Sabrina Geraci-Yee and Christopher Brianik wrote the draft article. All authors edited and approved the final version of this paper.

Acknowledgements

The study was supported by project R/FBM-36 funded by the National Sea Grant College Program of NOAA to the Research Foundation of State University of New York on behalf of New York Sea Grant. The work was also partially supported by grant #2016-70007-25759 funded by the United States Department of Agriculture, and by funding from the New York State Department of Environmental Conservation. We thank Drs. Eugene Burreson and Ryan Carnegie for providing clams that served us to generate the Virginia isolate of M. quahogii. We acknowledge the contributions of Dr. Roxanna Smolowitz to the understanding of QPX biology and for providing expert feedback on an earlier draft of this manuscript. We also recognize the technical support provided by former members of the Marine Animal Disease Laboratory at Stony Brook University, particularly Kailai Wang, Mickael Perrigault and Qianqian Liu. Finally, we would like to acknowledge Ishan Wankavala for his artwork used in the graphic depiction of the QPX life cycle.

Appendix A. Supplementary Data

Supplementary material related to this article can be found, in the online version, at doi:https://doi.org/10.1016/j.protis.2021.125793.

References

Anderson RS, Kraus BS, McGladdery SE, Reece KS, Stokes NA (2003) A thraustochytrid protist isolated from *Mercenaria mercenaria*: molecular characterization and host defense responses. Fish Shellfish Immunol **15**:183–194

Beakes GW, Thines M, Honda D (2015) Straminipile "Fungi" - Taxonomy. eLS. John Wiley & Sons, Ltd. pp1–9

Bower SM (1987a) *Labyrinthuloides haliotidis* n. sp. (Protozoa: Labyrinthomorpha), a pathogenic parasite of small juvenile abalone in a British Columbia mariculture facility. Can J Zool **65**:1996–2007

Bower SM (1987b) The life cycle and ultrastructure of a new species of thraustochytrid (Protozoa: Labyrinthomorpha) pathogenic to small abalone. Aquaculture **67**:269–272

Bowie PD (1970) The Isolation and Characterization of *Thraustochytrium pachydermum* from the Salton Sea, California, Department of Biological Sciences. The University of Arizona. M.Sc. thesis, 40p

Brothers C, Marks IIIE, Smolowitz R (2000) Conditions affecting the growth and zoosporulation of the protistan parasite QPX in culture. Biol Bull-US **199**:200–201

Burge CA, Kim CJ, Lyles JM, Harvell CD (2013) Special issue oceans and humans health: the ecology of marine opportunists. Microb Ecol **65**:869–879

Casadevall A, Steenbergen JN, Nosanchuk JD (2003) 'Ready made' virulence and 'dual use' virulence factors in pathogenic environmental fungi — the *Cryptococcus neoformans* paradigm. Curr Opin Microbiol **6**:332–337

Collado-Mercado E, Radway JC, Collier JL (2010) Novel uncultivated labyrinthulomycetes revealed by 18S rDNA sequences from seawater and sediment samples. Aquat Microb Ecol **58**:215–228

Collier JL, Geraci-Yee S, Lilje O, Gleason FH (2017) Possible impacts of zoosporic parasites in diseases of commercially important marine mollusc species: part II. Labyrinthulomycota. Bot Mar **60**:409–417

Dahl SF, Allam B (2007) Laboratory transmission studies of QPX disease in the northern quahog (= hard clam): development of an infection procedure. J Shellfish Res **26**: 383–389

Dahl SF, Perrigault M, Allam B (2008) Laboratory transmission studies of QPX disease in the hard clam: interactions between different host strains and pathogen isolates. Aquaculture **280**:64–70

Dahl SF, Perrigault M, Liu Q, Collier JL, Barnes DA, Allam B (2011) Effects of temperature on hard clam (*Mercenaria mercenaria*) immunity and QPX (Quahog Parasite Unknown) disease development: I. Dynamics of QPX disease. J Invertebr Pathol **106**:314–321

Doi K, Honda D (2017) Proposal of *Monorhizochytrium globosum* gen. nov., comb. nov. (Stramenopiles, Labyrinthulomycetes) for former *Thraustochytrium globosum* based on morphological features and phylogenetic relationships. Phycol Res **65**:188–201

Dove ADM, Bowser PR, Cerrato RM (2004) Histological analysis of an outbreak of QPX disease in wild hard clams *Mercenaria mercenaria* in New York. J Aquat Anim Health **16**: 246–250

Drinnan RE, Henderson EB (1963) 1962 mortalities and a possible disease organism in Neguac quahaugs. Biological Station at St. Andrews, Annual Report B11, St. Andrews, New Brunswick

Ford SE, Kraeuter JN, Robert DB, Mathis G (2002) Aquaculture-associated factors in QPX disease of hard clams: density and seed source. Aquaculture **208**:23–28

Ganuza E, Yang S, Amezquita M, Giraldo-Silva A, Andersen RA (2019) Genomics, biology and phylogeny *Aurantiochytrium acetophilum* sp. nov. (Thraustrochytriaceae), including first evidence of sexual reproduction. Protist **170**:209–232

Garcia-Vedrenne AE, Groner M, Page-Karjian A, Siegmund GF, Singhal S, Sziklay J, Roberts S (2013) Development of genomic resources for a thraustochytrid pathogen and investigation of temperature influences on gene expression. PLoS ONE **8**:e74196

Gast RJ, Moran DM, Audemard C, Lyons MM, DeFavari J, Reece KS, Leavitt D, Smolowitz R (2008) Environmental distribution and persistence of Quahog Parasite Unknown (QPX). Dis Aquat Org **81**:219–229

Geraci-Yee S, Allam B, Collier JL (submitted) Labyrinthulomycotan Pathogens of Marine Mollusks. In Freeman M (ed) Aquaculture Parasitology. Elsevier, Amsterdam, Netherlands.

Hassett BT (2020) A widely distributed thraustochytrid parasite of diatoms isolated from the Arctic represents a gen. and sp. nov. J Eukaryot Microbiol **67**:480–490

Hassett BT, Gradinger R (2018) New species of saprobic Labyrinthulea (=Labyrinthulomycota) and the erection of a gen. nov. to resolve molecular polyphyly within the aplanochytrids. J Eukaryot Microbiol **65**:475–483

Iwata I, Kimura K, Tomaru Y, Motomura T, Koike K, Koike K, Honda D (2017) Bothrosome formation in *Schizochytrium aggregatum* (Labyrinthulomycetes, Stramenopiles) during zoospore settlement. Protist **168**:206–219

Jeh E-J, Kumaran RS, Hur B-K (2009) Lipid body formation by *Thraustochytrium aureum* (ATCC 34304) in response to cell age. Korean J Chem Eng **25**:1103–1109

Jones EBG, Alderman DJ (1971) *Althornia crouchii* gen. et sp. nov., a marine biflagellate fungus. Nova Hedwigia **21**:3–4

Kleinschuster SJ, Smolowitz R, Parent J (1998) *In vitro* life cycle and propagation of Quahog Parasite Unknown. J Shellfish Res **17**:75–78

Kumar S, Stecher G, Li M, Knyaz C, Tamura K (2018) MEGA X: Molecular Evolutionary Genetics Analysis across computing platforms. Mol Biol Evol **35**:1547–1549

Leander CA, Porter D, Leander BS (2004) Comparative morphology and molecular phylogeny of aplanochytrids. Europ J Protistol **40**:317–328

Liu Q, Allam B, Collier JL (2009) Quantitative real-time PCR assay for QPX (Thraustochytriidae), a parasite of the hard clam (*Mercenaria mercenaria*). Appl Environ Microbiol **75**:4913–4918

Lyons MM, Smolowitz R, Uhlinger KR, Gast RJ, Ward JE (2005) Lethal marine snow: Pathogen of bivalve mollusc concealed in marine aggregates. Limnol Oceanogr **50**:1983–1988

Maas PAY, Kleinschuster SJ, Dykstra MJ, Smolowitz R, Parent J (1999) Molecular characterization of QPX, a pathogen of *Mercenaria mercenaria*. J Shellfish Res **18**:561–567

Medlin L, Elwood HJ, Stickel S, Sogin ML (1988) The characterization of enzymatically amplified eukaryotic 16S-like rRNA-coding regions. Gene **71**:491–499

Pandey A, Bhathena Z (2014) Prevalence of PUFA rich thraustochytrids sps. along the coast of Mumbai for production of bio oil. J Food Nutr Res **2**:993–999

Perkins FO (1972) The ultrastucture of holdfasts,' rhizoids', and' slime tracks' in thraustochtyriaceous fungi and *Labyrinthula* spp. Arch Mikrobiol **84**:95–118

Perrigault M, Bugge DM, Allam B (2010) Effect of environmental factors on survival and growth of quahog parasite unknown (QPX) *in vitro*. J Invertebr Pathol **104**:83–89

Perrigault M, Dahl SF, Espinosa EP, Gambino L, Allam B (2011) Effects of temperature on hard clam (*Mercenaria mercenaria*) immunity and QPX (Quahog Parasite Unknown) disease development: II. Defense parameters. J Invertebr Patho **106**:322–332

Pozarowski P, Darzynkiewicz Z (2004) Analysis of Cell Cycle by Flow Cytometry. In Schonthal AH (ed) Methods in Molecular Biology, vol. 281, Checkpoint Controls and Cancer **Vol 2**. Activiation and Regulation Protocols. Humama Press Inc., Totowa, NJ, pp 301–311

Ragan MA, MacCallum GS, Murphy CA, Cannone JJ, Gutell RR, McGladery SE (2000) Protistian parasite QPX of hard-shell clam *Mercinaria mercinaria* is a member of Labyrinthulomycota. Dis Aquat Org **42**:185–190

Raghukumar S (2002) Ecology of the marine protists, the Labyrinthulomycetes (Thraustochytrids and Labyrinthulids). Europ J Protistol **38**:127–145

Raghukumar S, Schaumann K (1993) An epifluorescence microscopy method for direct detection and enumeration of the fungi like marine protist, the thraustochytrids. Limnol Oceanogr **38**:182–187

Ragone-Calvo LM, Walker JG, Burreson EM (1998) Prevalence and distribution of QPX, Quahog Parasite Unknown, in hard clams *Mercenaria mercenaria* in Virginia, USA. Dis Aquat Org **33**:209–219

Rubin E, Pales Espinosa E, Koller A, Allam B (2015) Characterisation of the secretome of the clam parasite. QPX. Int J Parasitol **45**:187–196

Rubin E, Tanguy A, Espinosa EP, Allam B (2017) Differential gene expression in five isolates of the clam pathogen, quahog parasite unknown (QPX). J Eukaryot Microbiol **64**:647–654

Rubin E, Werneburg GT, Pales Espinosa E, Thanassi DG, Allam B (2016) Identification and characterization of peptidases secreted by quahog parasite unknown (QPX), the protistan parasite of hard clams. Dis Aquat Org **122**:21–33

Smolowitz R (2018) A review of QPX disease in the northern quahog(= hard clam) *Mercenaria mercenaria*. J Shellfish Res **37**:807–819

Smolowitz R, Leavitt D, Perkins F (1998) Observations of a protistan disease similar to QPX in *Mercenaria mercenaria* (hard clams) from the coast of Massachusetts. J Invertebr Pathol **71**:9–25

Stokes NA, Calvo LMR, Reece KS, Burreson EM (2002) Molecular diagnostics, field validation, and phylogenetic analysis of Quahog Parasite Unknown (QPX), a pathogen of the hard clam *Mercenaria mercenaria*. Dis Aquat Org **52**:233–247

Teske A, Ramsing NB, Habicht K, Fukui M, Kuver J, Jorgensen BB, Cohen Y (1998) Sulfate-reducing bacteria and their activities in cyanobacterial mats of solar lake (Sinai, Egypt). Appl Environ Microbiol **64**:2943–2951

Thompson JD, Higgins DG, Gibson TJ (1994) CLUSTAL W: improving the sensitivity of progressive multiple sequence alignment through sequence weighting, position specific gap penalties and weight matrix choice. Nucleic Acids Res **22**:4673–4680

Tsu CKM, Fan KW, Chow RKK, Jones EBG, Vrijmoed LLP (2012) Zoospore production and motility of mangrove thraustochytrids from Hong Kong under various salinities. Mycoscience **53**:1–9

Ueda M, Nomura Y, Doi K, Nakajima M, Honda D (2015) Seasonal dynamics of culturable thraustochytrids (Labyrinthulomycetes, Stramenopiles) in estuarine and coastal waters. Aquat Microb Ecol **74**:187–204

Whyte SK, Cawthorn RJ, McGladdery SE (1994) QPX (Quahaug Parasite X), a pathogen of northern quahaug *Mercenaria mercenaria* from the Gulf of St. Lawrence, Canada. Dis Aquat Org **19**:129–136

Yokoyama R, Honda D (2007) Taxonomic rearrangement of the genus *Schizochytrium* sensu lato based on morphology, chemotaxonomic characteristics, and 18S rRNA gene phylogeny (Thraustochytriaceae, Labyrinthulomycetes): emendation for *Schizochytrium* and erection of *Aurantiochytrium* and *Oblongichytrium* gen. nov. Mycoscience **48**:199–211

Yokoyama R, Salleh B, Honda D (2007) Taxonomic rearrangement of the genus *Ulkenia* sensu lato based on morphology, chemotaxonomical characteristics, and 18S rRNA gene phylogeny (Thraustochytriaceae, Labyrinthulomycetes): emendation for *Ulkenia* and erection of *Botryochytrium*, *Parietichytrium*, and *Sicyoidochytrium* gen. nov. Mycoscience **48**:329–341